Interferometry Lab Report (Revised)

Aditya Gautam
Sen Yuan

Department of Physics, University of Toronto
PHY324: Practical Physics II

December 9, 2024

Abstract

We conduct three experiments to measure the wavelength of the light emitted by a green laser, and then use that laser to find the index of refraction of a Plexiglas plate and the rate of thermal expansion for an aluminum rod, using a Michelson interferometer. We also attempted to do this for an incoherent light source. Our experimentation yields the following results: green laser wavelength: $540 \pm 40\ nm$; index of refraction: 1.5 ± 0.1; and coefficient of (linear) thermal expansion: $(2.7 \pm 0.4) \times 10^5\ K^{-1}$, all of which seem to be similar to and within the error margin for the known values for the same (See Discussion). We were unable to observe fringing for a red LED (incoherent source of light).

1 Introduction

Background Theory: Michelson Interferometers

Light interferes with itself due to its wave-particle nature and principles of quantum mechanics. Interference can be observed by varying the wavefront or amplitude of two light sources, and in this experiment, we use a Michelson interferometer to see the *amplitude* interference.

The interference pattern we observe in Figure 6 (Appendix) happens due to variations in the constructive & destructive interference as we move away from the central fringe. This is directly a result of the difference in amplitude of the two light sources.

The experiment uses a diverging lens to create interfering wavefronts. The difference in path lengths traveled results in the amplitude of the wavefronts being different, resulting in the pattern. The center of the pattern formed on the screen should be unaffected by divergence from the lens, so a change from light to dark of the central fringe or vice versa happens when the two wavefronts differ by half of the wavelength. We call one such change a fringe variation.

Instead of measuring minuscule distances of the order of the wavelength of light, we observe the total number of fringe variations over a larger distance moved by the lens and use it to calculate the wavelength by the equation

$$N\lambda = 2\Delta x \ , \tag{1}$$

where N is the number of fringe variations observed for incident light of wavelength λ when the Michelson interferometer has a $2\Delta x$ relative change in path length for the two sources.

The coherence length of a light source is the maximum path length difference (from zero) for which we can still observe the interference patterns. This is relatively large for a laser as the wavelength emitted is consistent. Excitation and de-excitation (which results in the emission) of particles in the laser medium, which have fixed energy states, emit consistent amounts of energy and thus coherent photons. LEDs are much more incoherent as the electrons crossing the semiconductor junctions in the diode are less consistent. So, interference is observable for larger path length differences for lasers than LEDs.

Index of Refraction

A block of transparent/translucent medium, if made consistently, has a specific way in which it affects light passing through it. Depending on the change of index of refraction from one medium to another, it causes light to go slower or faster, and results in a lateral shift.

Then by using an equation, we can observe the change in the interference pattern from tilting a medium which is rectangular, as the more angled it gets, the less it causes light to bend, changing the path length by a certain amount. If rotating the plate of thickness t by θ radians results in N fringe variations, then we can use the following equation to get the index of refraction of the plate as:

$$n = \frac{\left(\frac{N\lambda}{2t} + \cos\theta - 1\right)^2 + \sin^2\theta}{2\left(1 - \cos\theta - \frac{N\lambda}{2t}\right)} \ . \tag{2}$$

We can then make a linear approximation for small angles ($\theta << 1 : cos(\theta) \sim 1\, ,\, sin(\theta) \sim 0$) to simplify (1) as

$$N \simeq \frac{t}{\lambda}\theta^2 \left(1 - \frac{1}{n}\right) . \tag{3}$$

Thermal Expansion of Aluminium

It is hard to measure really small changes in length, but we now have a metric that corresponds to a small change in length. If we attach a mirror to the end of a rod, restrict its direction of expansion, and observe interference patterns from the mirror in a Michelson interferometer, we would see fringe variation corresponding to change in length with a resolution of the path length of the light interfering.

We can model linear thermal expansion as an exponential equation:

$$L = L_0 \, e^{\alpha \Delta T}, \tag{4}$$

where L_0 is the length at room temperature, ΔT is the change in temperature in K, L is the expanded length, and α is the coefficient of linear thermal expansion (**CLTE**). For the temperatures we observe, we can make a linear approximation and use (4) to get the following equation:

$$N \simeq \frac{2L_0}{\lambda} \alpha \Delta T \, . \tag{5}$$

2 Methods

Experimental Setup

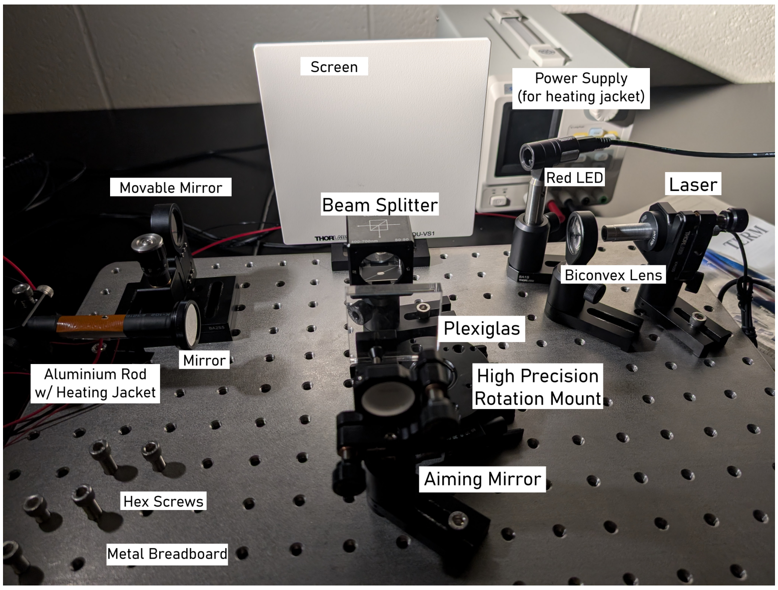

Figure 1: Experimental Setup for the interferometry experiment. Depending on the sub-part, we swap the Aluminium rod mirror with the movable mirror, and insert or remove the Plexiglas plate.

Our setup is based on the Thorlabs Michelson Interferometer Educational Kit [3] using a metal breadboard with threads for quarter-inch 20-cap hex screws & respective screwdriver. We mount our following components using magnetic mounts with locking mechanisms for the screws: white plastic screen, a green laser, a red LED, a rectangular Plexiglas plate, a plastic screen, a biconvex lens, a 50:50 non-polarizing beam splitter (CCM1-BS013 400-700 nm), a variable DC power supply (SIGLENT SPD1168X) a fixed power supply for the laser (5V DC), a high precision rotation mount with an attached plate holder. We used three mirrors: One for aiming, one movable with a micron adjustment dial, and one attached to an aluminum rod with a heating jacket. We also used iGaging EZCal calipers and a G1710 Greisinger Thermometer.

For experimentation, first, we placed the movable mirror squarely on the breadboard in one corner. Then, we mounted the laser roughly 30 cm away from the mirror and aimed it at its center. We tilted the beam so that the reflection formed on the center of the laser. To finish this segment, we moved the laser until the beam was centered on the mirror and locked it.

Halfway between the two, we placed the beam splitter. We locked the screen on the side where the beam splitter image forms. From there, we made sure the reflection from the beam splitter on the laser was also in the same spot as the one from the movable mirror, and the beam's image was in the center of the total image formed by the splitter on the screen.

We then placed the aiming mirror opposite the screen. We measured the rough distance between the movable mirror and beam splitter (measured either from the edge or from the center of the splitter and replicated for the other) and placed the aiming mirror roughly that much distance away from it. Then, we aimed the aiming mirror until the reflection on the screen laid precisely on the reflection from the movable mirror through the beam splitter.

Afterward, we introduced the bifocal lens and ensured the beam passed through the center of the lens. Then, we observed some fringes. From there, we moved the aiming mirror back or forth to maximize the size of the central fringe. Once the maximum achievable pattern was found (roughly one fringe), we locked the aiming mirror. Lastly, we placed the high-precision rotation mount between the splitter and the aiming mirror.

Data Collection

For wavelength measurement, we took measurements for fringe variation while moving the movable mirror using its knob. We ensured that we took data for multiple N values and started at the same zero each time, as the knob connection with the mirror may not be consistent for all positions.

For the index of refraction, we placed the plate in the mount and rotated it to find the maxima/largest central fringe. This was the zero angle for which the plate was perpendicular to the beam. We then slowly rotated the mount for some N fringes and recorded data for how much we deviated from the zero. We also recorded the thickness of the plate using calipers (averaged from different positions, came out as $7.71 \pm 0.01mm$).

We checked for both positive and negative displacement for both experiments to have an even spread of data which represents the setup fairly.

For CLTE of aluminium, we replaced and redid the procedure for the movable mirror with the aluminum rod with the mirror and heating jacket. Then, once we saw a significantly large central fringe, we turned on the thermometer to measure the room temperature (not needed for calculations, but a good benchmark for consistency). Then, we placed it inside the aluminium rod (shaped like a hollow cylinder). Lastly, we turned on the supply to the heating jacket and measured the fringe and temperature variations to see the correlation. The jacket and the cavity ensure expansion happens roughly linearly.

In our data collection for aluminium, we observed that turning off the power supply resulted in the fringes stopping generating and moving in the opposite direction (starting cooling from atmospheric temperature). For each data point, we started the temperature at the lowest measurement observed in the thermometer and took the ending one as the maximum observed in the thermometer (even after some stopping of the power supply).

Data analysis was done using NumPy and SciPy in Python 3.11.9. As all the equations we used to model the phenomena in our experiment were linear (See Introduction), we fit them to a linear function $y = mx + b$.

3 Results

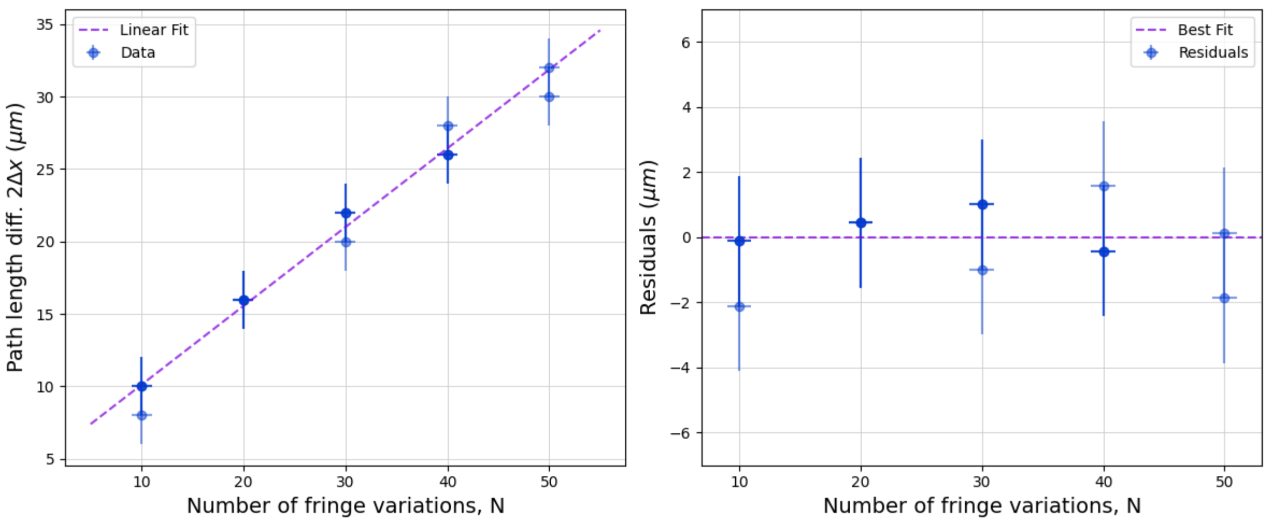

Figure 2: For wavelength calculation, a plot of measured relative path length difference (nm) vs. fringe variations observed (counts). Data (blue) is plotted with line of best fit (purple). Slope represents $2\Delta x/\Delta N = \lambda$. Line of best fit has slope 0.54 ± 0.04 μm per count with offset 4.7 ± 1.1 μm. Resultant wavelength is $\lambda = 540 \pm 40$ nm. Plot has reduced $\chi^2 = 0.24$ and probability 0.9. Chi values and unpatterned residual indicate that the fit is decent. Note that there are multiple measurements for N values due to absolute values taken and multiple measurements are indicated by darker markers.

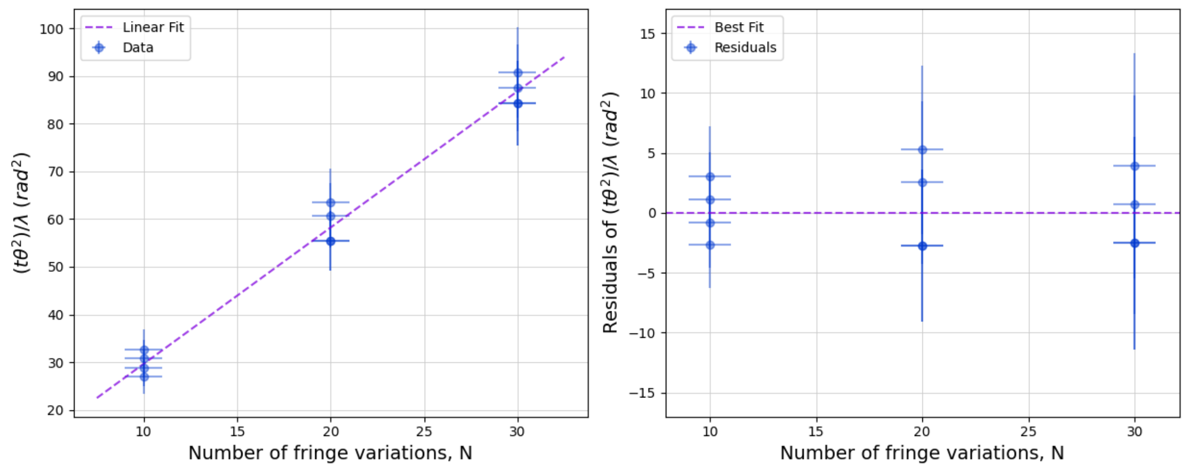

Figure 3: Index of refraction calculation: a plot of a variable of thickness, angle(rad), and incident wavelength (units rad^2) vs. fringe variations observed (counts). Data (blue) is plotted with line of best fit (purple) with residuals. Slope represents $(1 - 1/n)$. Line of best fit has slope 2.9 ± 0.2 (rad^2) per count with offset 1.0 ± 3.6 (rad^2). Resultant index of refraction is $n = 1.5 \pm 0.1$. Plot has reduced $\chi^2 = 0.23$ and probability 1.0. Chi values indicative of over-fitting, probably due to repetitive measurements for the same N variations. Reasonable chi values and unpatterned residual indicate that the fit is good.

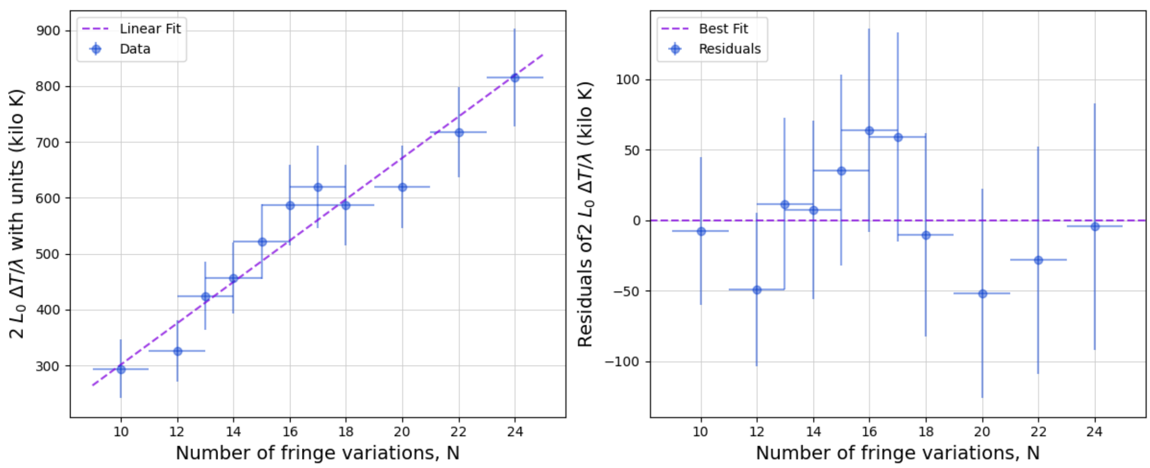

Figure 4: For the CLTE of aluminium calculation, a plot of measured variable of base length, change in temperature and incident wavelength (units (kK)) vs. fringe variations observed (counts). Data (blue) is plotted with line of best fit (purple). Slope represents $1/\alpha$. Line of best fit has slope 37.0 ± 5.1 kK per count with offset -70 ± 80 kK. Resultant CLTE is $\alpha = (2.7 \pm 0.4) \times 10^{-5}$ K^{-1}. The plot has reduced $\chi^2 = 0.32$ and probability 0.95. Reasonable chi values and unpatterned residual indicate that the fit is decent.

4 Discussion

For the green laser, the equipment manual [3] lists the output wavelength to be 532 nm, which is very close to and within the error margin of 540 ± 40 nm (from our experiment). For the Plexiglas plate, the index of refraction of polymethyl methacrylate (PMMA/Plexiglas) is known to be around 1.5 for light of wavelength of 590nm from Wikipedia which sources a refractive index database [4]. This is again close to and within the error margin of our calculated value 1.5 ± 0.1. Lastly, the CLTE for aluminium is known to be around 2.3×10^{-5} K^{-1}, which also lies within error margins for our calculated value of $(2.7 \pm 0.4) \times 10^{-5}$ K^{-1}. The known value was obtained from the Advanced Mechanical Engineering solutions database [5]. The closeness of the obtained values to the known ones validate our experimental design to some extent.

Sources of Error and Uncertainty Calculations

Every device we use to measure data has a resolution (or least count). The calipers had a least count of 0.01 mm, movable mirror knob had a least count of 1 micron, the rotation mount had a least count of 5 minutes, and the thermometer has a percentage error that we round up to the resolution of the measurement (0.1 K) as listed in its Datasheet [6]. All these were used as uncertainties for the calculations (See sample calculation in appendix).

Our sources of error do exist, but we claim that their extents were minimized by our experimental design and are accounted for in the uncertainty margins.

In the wavelength calculation, we did see some repeated results for the same N fringe variations, but sometimes we did not as instead of having a large spread, we did multiple trials to see the validity of the measurement. The knob of the movable mirror seemed to have some inconsistency, as each fringe variations happened for some fraction of a micron (least count of the knob). Thus, we took multiple measurements and left it to the linear regression (SciPy curve_fit) to account for the line of best fit instead of taking their average.

One of the core measurements we make is fringe variations. We counted these manually by having two people watch the pattern change. We consider a ± 1 uncertainty to the count from two things: One, some possible level of miscounting. Two, the fractional fringe changes/phase difference. We do not exactly know what phase we start and end at but know that we have some N fringe variations with some less/more, we account for that in the uncertainty as well.

Furthermore, it seemed there was an offset for the line plotted. We claim this was was due to the interlocking of the gears being imperfect initially, and then being smoother once the rotation starts. This may be due to some gap or connection issue with the springs or teeth of the gears as it converts a rotating knob to linear translation of the mirror. Our model ignores this offset as we consider the slope of the curve and not the exact value. Also we started the measurement from the same position of the knob each time to have a notion of consistency.

Heat and vibrations (to the breadboard and unevenly to the optic components) from ambient sources also caused observed changes in interference, but to a minimal/non-influential level, only causing minor distortions instead of counting errors for the fringe variations. This was due to the hotter air having lower optical density than the colder air. We tried to minimize this by minimizing contact with the table, keeping body parts away from path of the beam, and covering our mouths to avoid air currents.

Minor irregularities in the construction of the optic components may also affect the measurements, but we assumed them to be constant for the sake of this experiment, as the light beam passes through a small fixed portion of components, and should affect the data by some change in amplitude/wavelength. This is very small, does not affect the measurements as we measure the relative path length difference not absolute path length. The same applies to index of refraction as well for relative change in angle.

The ambient heat of the room temperature and any irregularities in the current supplied to, or the contact with the rod, of the heat jacket may be considered, but should be within the propagated uncertainties. These mostly distort the image an we care more about variations rather than getting a perfectly circular image.

One thing specific to the thermal expansion coefficient calculation is the fact that we are trying to measure the CLTE and not a volume-based coefficient. The heating is provided to the rod radially inwards, and the rod has a hollow cavity for the thermometer. Some amount of expansion may happen outwards, which should be off-set by the jacket's confines, and some should be inwards but should be neutralized by the heat absorbed by the thermometer. As the value we compare is CLTE and not volume-expansion, as the rod is small, and there is atmospheric influence, we say the deviation due to these is accounted for in the uncertainty as the value found is reasonably close to known CLTE. Additionally, we do not know the exact alloy/mix of aluminium used in the setup, and we know these have different CLTE values [5].

Lastly, there may be some errors due to imperfect pathways for the setup of the optical devices, as if they deviate by a little, the interference may not be consistent. On a broader scale, this should not affect the setup much, and we tried to minimize this by centering the beam for each of the components as much as we could.

Red LED

The main goal of the red LED experiment was to calculate the coherence length of the same. Coherence length related to the rough length of the spectrum which has a significantly non-zero intensity from the light source.

An LED has a much larger spectrum compared to a laser due to the construction. As a result, as the light propagates, the wavelengths deviate and vary, resulting the spectrum flattening-out. For a laser, as this is very thin and sharp peak, the pattern changes very little over distances, meaning the light stays coherent for a large distance, and has a large coherence length.

On the other hand, LEDs have a much wider spectrum, which spreads out and nearly flattens. As a result, the coherence length is much shorter. as it approaches a broad spectrum

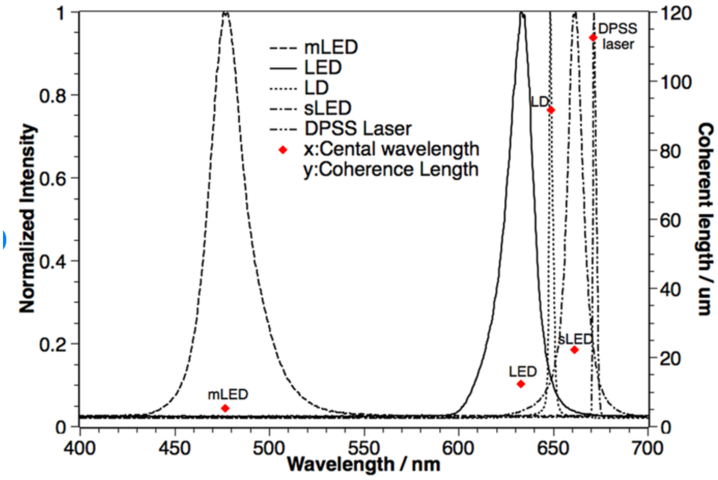

Figure 5: Coherence lengths (red dots) of different light sources [2]. Note the very small coherence lengths for the LEDs compared to the much larger ones for the LD and the laser.

Why this is relevant is that the longer the light travels, the wavelength output becomes more and more varied. As Michelson interferometers depend on amplitude-based interference, different wavelengths vary differently due to different frequencies, and create a flat pattern, where interference *does* happen, but is so small that it is invisible to the human eye. We think the provided red LED potentially had a very small coherence length that we could not find the 'sweet-spot' for in the given time frame. It may also be some factor of the setup provided that we were unaware of. The laser provided is also collimated, while the LED is not, but we do not expect this to have as much of an effect as the coherence.

5 Conclusion

We were successful in conducting most of our experiments, except for the red LED coherence length calculation. Our setup used the Michelson interferometer to calculate the value for wavelength of green laser as $540 \pm 40\ nm$. We further used that to calculate index of refraction for a Plexiglas plate 1.5 ± 0.1 and the thermal expansion coefficient for an aluminium rod $(2.7 \pm 0.4) \times 10^{-5}\ K^{-1}$. Known values (Refer to Discussion) for these variables lie within the error margins of their experimentally obtained counterparts. This shows the reliability of the Michelson interferometer for calculating small changes in length measurement using a coherent source of light.

6 References

[1] Wilson, B. (2024). *Interferometry Lab Manual* (Revision: 63bbf38, dated August 29, 2024). https://www.physics.utoronto.ca/ phy224_324/LabManuals/Interferometers.pdf

[2] Deng, Y. & Chu, D. (2017). Coherence properties of different light sources and their effect on the image sharpness and speckle of holographic displays. *Scientific Reports 7*, Article 1. https://doi.org/10.17863/CAM.10354.

[3] https://www.thorlabs.com/newgrouppage9.cfm?objectgroup_id=10107 - Accessed December 3, 2024

[4] https://en.wikipedia.org/wiki/Poly(methyl_methacrylate) - Accessed December 3, 2024

[5] https://amesweb.info/Materials/Linear-Thermal-Expansion-Coefficient-Metals.aspx - Accessed December 3, 2024

[6] https://www.automation24.biz/thermometer-greisinger-g-1710-609828 - Accessed December 3, 2024

7 Acknowledgment of AI Use

The authors used Grammarly for removing any spelling and grammatical errors in the content, and ChatGPT to generate the LaTeX code for the preamble to import packages, figure placement, and document formatting.

The authors of this paper did not use any AI tools for generating the content, data analysis, the experimental design, or any other aid other than the ones listed above.

Appendix

Additional Figures

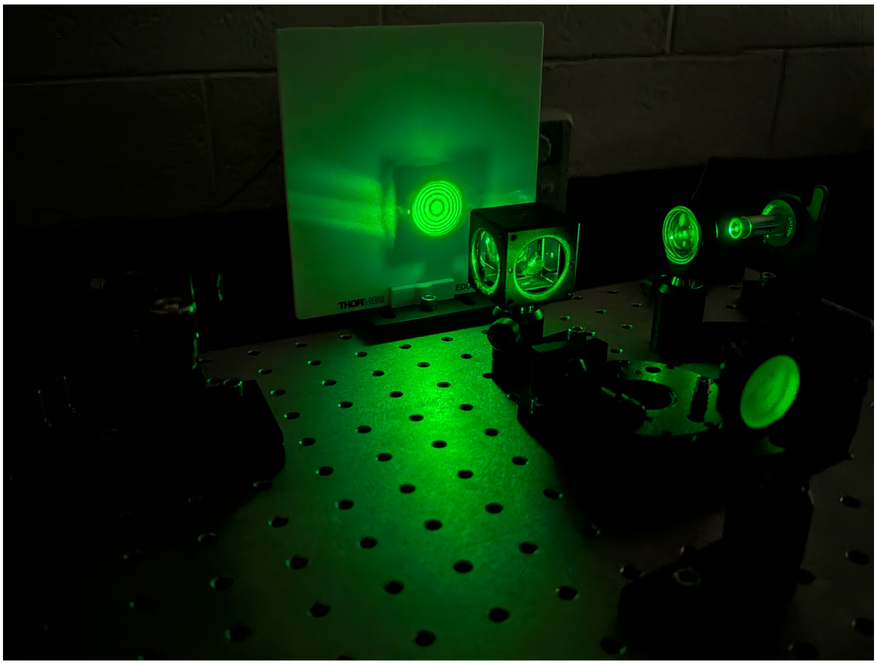

Figure 6: Sample Interference pattern from the setup.

Sample Uncertainty Calculation:

Sample calculation for the green wavelength: (acquired through diagonal of the pcov matrix, explained here)

Fringe variations 1 = 10 ± 1; $x_{10} = 5 \pm 1$
Fringe variations 2 = 20 ± 1; $x_{20} = 8 \pm 1$
Fringe variations 3 = 30 ± 1; $x_{30} = 10 \pm 1$

For the equation $N\lambda = 2\Delta x$; we get $\lambda = 2\frac{\Delta x}{\Delta N}$ as we expect the offset of the slope to be from the interlocking mechanism of the gears.

Thus $\lambda_1 = 2 * (8 - 5)/10 = 0.6$
and $\lambda_2 = 2 * (10 - 8)/10 = 0.4$

Propagating $\delta\lambda = \lambda(\frac{\delta\Delta x}{\Delta x} + \frac{\delta\Delta N}{\Delta N})$:

We get $\delta\lambda_1 = 0.6 * (2/3 + 2/10) = 0.5$ and $\delta\lambda_2 = \lambda_2(2/2 + 2/10) = 0.4$.

Noticing very large uncertainties, we instead use the average error uncertainty taken as:
$\bar{\lambda} = (1/n) \cdot \Sigma_{i=1}^{n} (\lambda_i) = 0.5$
$\Delta\bar{\lambda} = (1/n) \cdot \Sigma_{i=1}^{n} (\bar{\lambda} - \lambda_i) = 0.1$

So our final mock measurement comes out to be $\lambda = 0.5 \pm 0.1 \mu m$.

This was done on a larger scale with all the values we got for all three sub-experiments